FLEXIBLE MANUFACTURING FOR PHOTONICS DEVICE ASSEMBLY

Shin-yee Lu
Thrust Area Leader, Engineering Research Division, Engineering Department
Michael D. Pocha
Group Leader, Engineering Research Division, Engineering Department
Oliver. T. Strand
Physicist, L-Division, Nuclear Test Experimental Sciences Department
K. David Young
Project Engineer, Engineering Research Division, Engineering Department
Lawrence Livermore National Laboratory
P.O. Box 808
Livermore, CA 94550

The assembly of photonics devices such as laser diodes, optical modulators, and opto-electronics multi-chip modules (OEMCM), usually requires the placement of micron size devices such as laser diodes, and sub-micron precision attachment between optical fibers and diodes or waveguide modulators (usually referred to as pigtailing). This is a very labor intensive process. Studies done by the opto-electronics (OE) industry have shown that 95% of the cost of a pigtailed photonic device is due to the use of manual alignment and bonding techniques, which is the current practice in industry. At Lawrence Livermore National Laboratory, we are working to reduce the cost of packaging OE devices through the use of automation. Our efforts are concentrated on several areas that are directly related to an automated process. This paper will focus on our progress in two of those areas, in particular, an automated fiber pigtailing machine and silicon micro-bench technology compatible with an automated process.

INTRODUCTION

At present, the cost of opto-electronic devices is dominated by the effort required to package those devices into an integrated system. Components such as laser diodes and modulators, designed for high-performance applications, are single-mode devices; they must be connected together using optical fibers or other type of waveguide with sub-micron alignment accuracies. Presently, the OE packaging is usually performed by highly skilled technicians looking through microscopes and manually adjusting sub-micron stages. For single mode fibers, six degrees of freedom for positioning are sometimes required. Once the alignment is correct, the components must be held in place using epoxy, solder, or other attachment techniques, and realigned before the gluing process is settled. This labor-intensive process results in only a few packages being produced per day by each technician. The packaging costs are by far the highest fraction of the total cost of an assembled OE package. The consequences of this low-volume labor-intensive process of packaging OE devices are readily apparent. The costs are too high to allow the advantages of fiber optics to penetrate such markets as on-chip interconnects, interboard connections in computers, and local area networks.

At LLNL, we believe that the packaging process must be automated to significantly reduce the costs of OE devices. The electronics industry has successfully reduced the costs of its products through the massive use of automation, including alignment, parts handling and feeding, and in-situ quality control. A simple model (Figure 1), which takes into account the initial cost of the automated machinery, the labor costs of an operator, and the material costs of the devices, shows that substantial cost savings may also be realized in the opto-electronics industry at even modest production rates. Unfortunately, the sub-micron precisions, and six-axis alignment required for OE packaging greatly exceeds the requirements of the electronics industry. The automated systems developed to assemble integrated circuits cannot be applied to the problem of packaging opto-electronic circuits.

Work was performed under the auspices of the U.S. Department of Energy by Lawrence Livermore National Laboratory under Contract W-7405-ENG-48.

6. R. G. Waters, R. J. Dalby, J. A. Baumann, J. L. De Sanctis and A. H. Shepard, "Dark-Line-Resistant Diode Laser at 0.8 μm Comprising InAlGaAs Strained Quantum Well", IEEE Photonics Technol. Lett. 3, 409 (1991).

7. S. L. Yellen, A. H. Shepard, R. J. Dalby, J. A. Baumann, H. B. Serreze, T. S. Guido, R. Soltz, K. J. Bystrom, C. M. Harding and R. G. Waters, "Reliability of GaAs-Based Semiconductor Diode Lasers: 0.6 - 1.1 μm", IEEE Jour. Quant. Elec. 29, 2058 (1993).

8. R. Beach, W. J. Benett, B. L. Freitas, D. Mundinger, B. J. Comaskey, R. W. Solarz and M. A. Emanuel, "Modular Microchannel Cooled Heatsinks for High Average Power Laser Diode Arrays", IEEE Jour. Quant. Elec. 28, 966 (1992).

9. W. J. Benett, B. L. Freitas, D. Ciarlo, R. Beach, S. Sutton, M. Emanuel and R. Solarz, "Microchannel cooled heatsinks for high average power laser diode arrays", Proc. SPIE 1865, 144 (1993).

10. R. Beach, private communication.

11. A. Karpinski and K. J. Linden, "Novel Packaging for High-Performance Low-Cost Diode Laser Arrays", OSA Tech. Digest 16 (Nov., 1990).

12. D. P. Bour, D. W. Treat, R. L. Thornton, T. L. Paoli, R. D. Bringans, B. S. Krusor, R. S. Geels, D. F. Welch and T. Y Wang, "Low threshold 633 nm, single tensile-strained quantum well GaInP/AlGaInP laser", Appl. Phys. Lett. 60, 1927 (1992).

13. S. J. Eglash and H. K. Choi, "Efficient GaInAsSb/AlGaAsSb Diode Lasers Emitting at 2.29 μm", Appl. Phys. Lett. 57, 1292 (1990).

14. H. K. Choi and S. J. Eglash, "High-power multiple-quantum-well GaInAsSb/AlGaAsSb diode lasers emitting at 2.1 μm with low threshold current density", Appl. Phys. Lett. 61, 1154 (1992).

15. S. Major, D. Nam, J. Osinki and D. Welch, "High power 2.0 μm InGaAsP laser diodes", IEEE Photonics Technol. Lett. 5, 594 (1993).

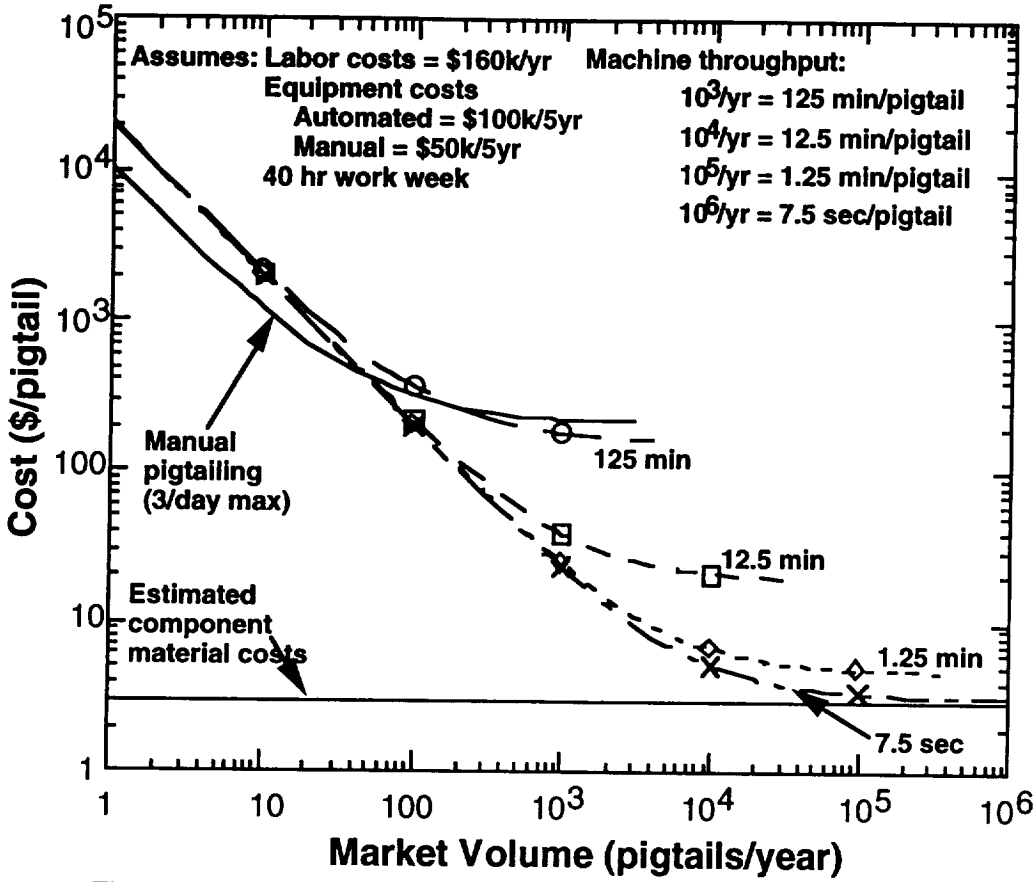

Figure 1. Cost Analysis of an Automated Opto-electronic Packaging Machine

We are currently designing and building a flexible workcell for automating the packaging of OE devices (Figure 2). The workcell design uses machine vision to provide position information for low resolution (microns) long travel movement, and optic power throughput optimization to provide final high resolution small travel alignment. The combined vision/optic power feedback approach provides a low cost output metrology for high resolution positioners. It also eliminates the need of high precision fixturing, calibration, and temperature control to hold photonics devices in fixed locations at micron precision. The workcell should be able to handle a wide variety of different sizes and attachment geometry of photonic devices.

The initial task is to align a single-mode fiber to each end of a Mach-Zehnder waveguide modulator (fiber pigtailing). We are also developing silicon micro-bench based techniques to provide a packaging technology that is compatible with automated alignment and pigtailing.

MACHINE VISION SYSTEM

There are several parameters that need to be considered in the design of a system for machine vision: pixel resolution, field of view (FoV) depth of field, and the cost. Ideally, the vision system should have high pixel resolution to yield position accuracy, large field of view to cover the entire size and depth range of the photonic device, and low cost. We decided to use a low cost, standard microscopic camera commonly used for industrial inspection. The image frame grabber produces 640-by-480 pixels in one view. The pixel resolution is 1.44 micron. The active view volume is approximately 900 x 700 x 100 cubic microns, which can be substantially smaller than a photonic device to be assembled. Currently, the automated packaging workcell consists of two microscopic camera systems that provide a top view and a side view of the substrate and the fibers. Each camera is mounted on motorized stages to cover the entire area of interest.

The motion control hardware and software for the vision system are chosen for position accuracy to be compatible with the image resolution such that the static position repeatability (without the use of vision feedback) of the vision system is 2 to 5 microns. There are two reasons for the high position repeatability requirement of the

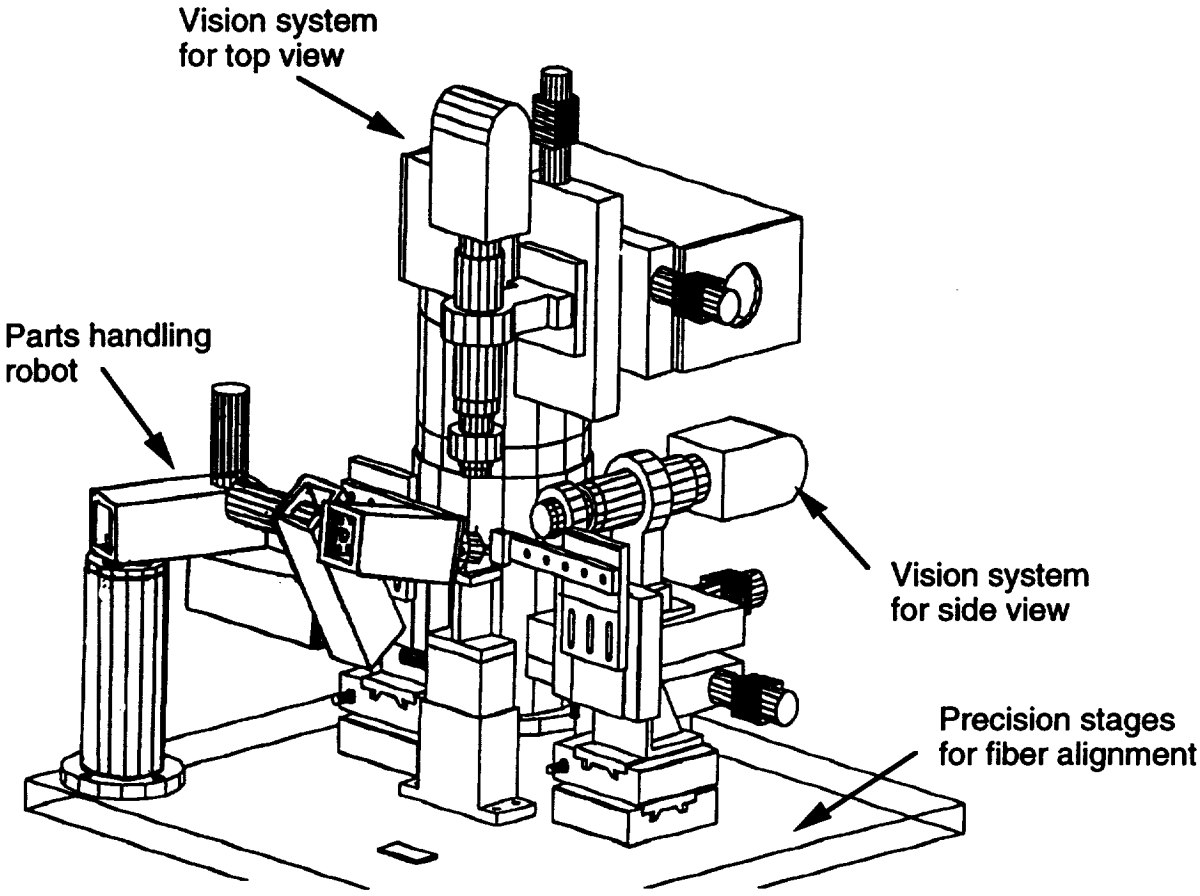

Figure 2. LLNL Automated Opto-electronics Packaging Machine

vision system: (1) to move from one FoV to the next along a certain trajectory, (2) to move between two focal planes, and be able to register the two coordinate systems defined by the two images.

The top camera system has three-degrees of freedom that are configured as a scalar arm to move around the horizontal plane -- one rotary motor swings the arm and one linear stage slides along the arm. The camera is mounted on another linear slide perpendicular to the arm to move along the optic axis. The rotary motor used in the top camera system has 600,000 counts per revolution. The rotary arm is ten inches long. Both sides have two inches travel and one micron repeatability. The repeatability of the top camera system is approximately 2.5 x 1 x 1 cubic microns. The side camera has two-degrees of freedom for moving along a horizontal line and for moving along the optic axis. The same type of slides are used for the side camera system.

VISION FEEDBACK FOR KINEMATIC CALIBRATION

The static position repeatability is a necessary but not a sufficient condition to register the coordinate systems defined by two FoV of two focal planes. The misalignment of the mechanic system also needs to be calibrated to generate the necessary parameters for coordinate transformation.[1,2] Since the side camera represents a subsystem of the top camera system (without the rotational degree of freedom), we will describe the calibration procedure using vision feedback to back-calculate the kinematic configuration of the top camera system only.

The calibration procedure utilizes a sequence of predetermined motions of the top camera system. Stationary fiducials on the substrate are tracked by their respective pixel coordinates in the sequence of focal plane images. Of the many kinematic parameters that can be calibrated, we concentrate on the following three: The misalignment angle of the Camera Frame with respect to Linear Stage Frame, δ, and the coordinates of the origin of the Camera Frame as measured in the Linear Stage Frame coordinate system, h and l. The orientation of the Linear Stage Frame is changed by a motor drive system through the control of the angular displacement, $\Delta\theta$. Fig. 3

illustrates the kinematic parameters and their relationships to the fiducials, the Camera Frame and Linear Stage Frame.

The misalignment angle is determined by moving the top camera along the linear stage translation axis, as measured by the Δl increments, while keeping the rotation degree of freedom fixed. The linear stage is commanded to move a small distance at a time while keeping the same set of fiducials in the field-of-view of the camera at all times. Selected points of the fiducials are tracked and their pixel coordinates on the focal plane image are registered. The misalignment angle is calculated from the pixel coordinates of a given fiducial point corresponding to its location before (x_1 and y_1) and after a commanded move (x_2 and y_2) by

$$\tan\delta = \frac{x_2 - x_1}{y_2 - y_1} \tag{1}$$

The coordinates of the image plane origin are determined by rotating the top camera while keeping the linear degree of freedom fixed. The motor drive is commanded to move in a small angle increments $\Delta\theta$, while the same set of fiducials are kept within the field-of-view. Again, selected points of the fiducials are tracked and their pixel coordinates on the image are registered. Using the following set of linear equations, the coordinates, h and l, are computed from the pixel coordinates of a given fiducial point corresponding to its location before (x_1 and y_1) and after the move (x_2 and y_2), the previously calculated misalignment angle, δ, and the angle increment, $\Delta\theta$.

$$\begin{aligned}(1-\cos\Delta\theta)l - \sin\Delta\theta h &= (y_1 - y_2\cos\Delta\theta - x_2\sin\Delta\theta)\cos\delta \\ &\quad +(x_1 - x_2\cos\Delta\theta + y_2\sin\Delta\theta)\sin\delta \end{aligned} \tag{2}$$

$$\begin{aligned}\sin\Delta\theta l + (1-\cos\Delta\theta)h &= (x_1 - x_2\cos\Delta\theta + y_2\sin\Delta\theta)\cos\delta \\ &\quad +(x_2\sin\Delta\theta - y_1 + y_2\cos\Delta\theta)\sin\delta \end{aligned} \tag{3}$$

SILICON MICRO-BENCH

At LLNL, we are also working on silicon micro-bench techniques such that all components of an opto-electronic multi-chip module (OEMCM) can be attached to flat substrates with direct access from the top. Thus, the process lends itself to a simple packaging procedure. The substrates consist of silicon with gold metalization pads to which the components are attached and the electrical connections are made. Unique polycrystalline silicon on-board heaters are used to quickly attach by reflowing solder the components and single mode fiber pigtails to sub-micron positioning tolerances.

Prototype silicon micro-benches were developed to pigtail high-powered 800 nm laser diodes to single mode fibers. These micro-benches are 13 mm long by 6 mm wide and 0.5 mm thick. The success of the prototype has led us to develop several follow-up designs. For example, the micro-bench shown in Figure 4 is for packaging a 1550 nm DFB laser. On the left side of the micro-bench, we photolithographically pattern various gold pads to provide a ground plane for the laser and stress relief pads for the wire bonds. For the fiber attachment on the other side of the micro-bench, we build two heating elements made of polysilicon which are attached to gold bonding pads to provide electrical contact points. In the center of each heater, we pattern a gold pad on a layer of silicon dioxide. This gold pad provides the solder attachment point while the silicon dioxide electrically isolates the gold pad from the polysilicon heater. The gold pads are 1 mm by 0.5 mm each and are sufficiently large to solder a 250 micron diameter fiber at the two attachment points. Presently, we use either 100-micron diameter solder balls or solder paste to attach the metalized fiber.

The performance of the polysilicon heaters on our prototype is very reproducible with a specially constructed power supply that allows us to accurately control the magnitude and time of the applied current. Fiber positioning is done by active alignment to sub-micrometer tolerances. While the fiber is held in the position that achieves maximum optical coupling, solder is reflowed to lock the fiber in place. We typically apply one amp of current for approximately 0.5 secs. to reflow solder at the fiber attachment points. We observe no decrease in the amount of light coupled from an 800 nm laser diode into a single-mode fiber before and after the solder reflow and cooling.

Our micro-bench geometries with on-board heaters allow rapid attachment of not only the fiber, but all other components to be placed on the micro-bench. Applying large currents for longer periods of time allows solder reflow at other locations on the micro-bench. Using solders with different melting temperatures and judiciously choosing the order of attachment allows a variety of components to be soldered to the micro-bench without movement of previously attached components. Generally, components furthest from the heater will be attached first using a high current through the heater. We can solder a thermoelectric cooler, a thermistor, and a laser diode onto our micro-bench at different distances from the heater in less than 15 minutes. The placement of these components does not require sub-micron alignment, and can therefore be aligned using standard techniques used in the electronics industry, which is heavily automated. We envision that the placement and soldering of these components onto the micro-benches could be performed by an automated system in only a few minutes.

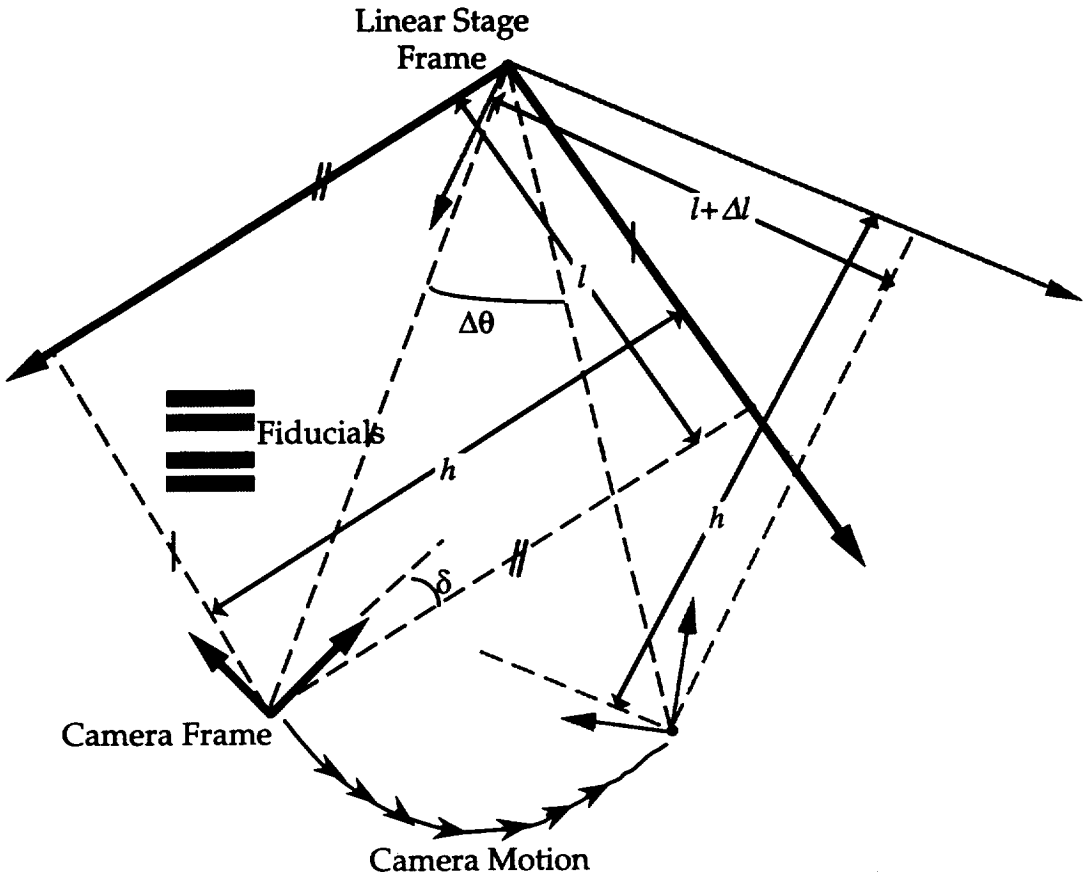

Figure 3. Top Camera System Kinematics

As the last step, the fiber must be aligned to sub-micron tolerances and is attached using the least amount of current through the heaters. The vision system is used to search for those soldered components and attachment points based on fudicial markings. Fiber placement and alignment is guided by the position information generated from computer vision programs to 2 to 5 micron precisions. The final sub-micron precision is provided by an optical power feedback system.[3]

The idea of on-board heaters lend itself to applications other than packaging laser diodes. We are presently designing a longer micro-bench with heaters at each end to pigtail both ends of a semiconductor optical amplifier. We are also investigating geometries compatible with high speed applications in which on-board transmission lines will be needed to provide sufficient bandwith.

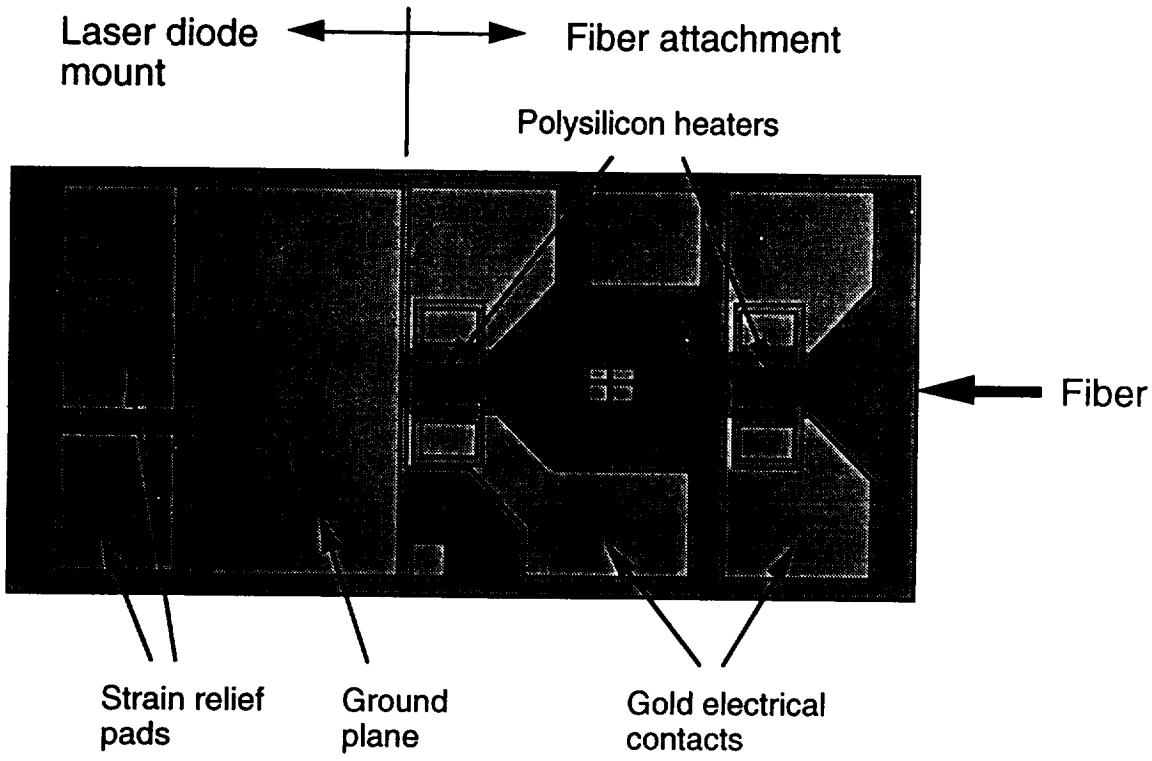

Figure 4. Sketch of our Micro-bench

SUMMARY

The key element in reducing the costs of packaged opto-electronic devices is to minimize the manual labor costs. According to our model, manual pigtailing techniques will not allow the cost of a pigtailed OE device to drop below approximately $250. On the other hand, an automated process could allow the costs to drop as low as $10 per pigtail--a factor of 25 decrease in cost. A fully automated system for fiber pigtailing must include automated fiber alignment, fiber attachment techniques which are compatible with an automated process, in-situ quality control, and automated parts handling and feeding. We present here our efforts in addressing the alignment issue and a fiber attachment technique. Variations of an automated system such as this could perform not only sub-micron active alignments as we discuss here, but also passive alignments using tactile feedback rather than optical feedback. The important point is to automate the process regardless of the alignment technique involved. We believe that a massive market is ready for the technology that opto-electronics can provide and is just waiting for the costs to be reduced.

ACKNOWLEDGEMENT

The authors would like to thank Mark Lowry for his guidance and support of the photonics packaging automated effort.

REFERENCES

(1) "Characterization and Pigtailing of Advanced Waveguide Devices using AutoAlign", Scott Jordan in collaboration with Lawrence Livermore National Laboratory, Newport Corporation Internal Report, April 1993.

(2) "Determination of Camera Location from 2D to 3D Line and Point Correspondences", Y. Liu, T. S. Huang, O. D. Faugeras, Proceedings of the IEEE Conference on Computer Vision and Pattern Recognition, June 1988.

(3) "Vision-based Automatic Theodolite for Robot Calibration", M. R. Driels, U. S. Pathre, IEE Trans. on Robotics and Automation, Vol. 7, No. 3, June 1991.